Acceleration and Parallelization of the Method of Characteristics for Lattice and Whole-Core Heterogeneous Calculations

Gil Soo Lee, Nam Zin Cho, and Ser Gi Hong

Korea Advanced Institute of Science and Technology
Department of Nuclear Engineering
373-1 Kusong-dong, Yusong-gu, Taejon, Korea 305-701
gslee@nurapt6.kaist.ac.kr; nzcho@sorak.kaist.ac.kr
hong@fermi.kaist.ac.kr

Abstract

The CRX code based on the method of characteristics extended to treat anisotropic scattering was accelerated with the coarse mesh rebalance (CMR) method for inner iteration and the coarse mesh/coarse group rebalance(CGR) method for outer iteration involved with the eigenvalue search. A parallelization scheme in angular domain rather than in spatial domain was also implemented for further reduction of the computing time. To effectively handle heterogeneous large scale problems, the original ray tracing scheme in the CRX code was modified to modular ray tracing so that all lattice cells have the same ray distribution for each direction. This modification reduces effectively the computer memory and computing time in the ray tracing. Therefore, it is possible to treat the large scale problems such as multi-assembly problems and whole core problems. The acceleration and parallelization methods were applied to several fuel assembly problems and a whole core problem to show their effectiveness. The numerical results show that they are effective in reducing the number of iterations and the computing time.

I. INTRODUCTION

The method of characteristics (MOC)([1],[2],[3],[4],[5],[6],[7],[8]) which combines desirable features of the integral transport and S_N methods has been considered as an effective methodology in the lattice calculation. This method gives accurate solutions in complex geometries, strong absorber problems, strongly anisotropic problems and so on, while its calculation preserves the simplicity of the S_N method. It divides directions like in S_N and for each direction performs transport calculation like the collision probability method by integrating the differential form of the within-group transport equation along its parallel characteristic lines. For better accuracy, it needs many rays and fine angle divisions. Like most of the transport methods, MOC also requires long computing times for scattering dominant problems and problems with significant upscattering. Therefore to reduce computing time, it needs to be accelerated. Although there are many acceleration techniques([9],[10],[11],[12]) in the discrete ordinates transport calculation, these methods cannot be applied directly or used effectively in the method of characteristics. Recently, the method of characteristics with a direct neutron path linking technique and with a domain decomposition parallel computing was applied to the multi-assembly problem[13].

In this paper, the coarse mesh rebalance (CMR) method [14], which uses the fact that converged solution must satisfy the neutron balance equation and can be easily implemented for various methods in general geometry was used for accelerating the inner iteration involved with the scattering source iteration. For eigenvalue problems, there are several ways to apply the coarse mesh rebalance method (e.g., whole-system group-wise, coarse mesh all-group-collapsed, and coarse mesh group-wise rebalance methods [15]). In this paper, a coarse mesh/coarse group rebalance method including the coarse mesh group-wise rebalance in particular was used to accelerate the outer iteration. With this coarse mesh/coarse group rebalance method, the rebalance equation leads to an equation that resembles a multigroup finite-differenced eigenvalue problem. Therefore, this equation must be solved with two iteration schemes (i.e., inner and outer iterations).

The CRX code ([1],[2]) has implemented these acceleration schemes and was also extended to treat anisotropic scattering. In the case of anisotropic scattering problems, the scattering source term must be carefully treated since its integration over the whole angular domain may not be zero depending on the used angular quadrature set [16]. To further reduce the computing time and save the computer memory, a parallelization scheme that does not require an iterative procedure was implemented by decomposing the angular domain. To handle the large scale problems including the multi-assembly and the whole core problems, the original ray tracing scheme was modified. The modified ray tracing scheme requires that all lattice cells have the same size and the angular quadrature set is selected so that all lattice cells have the same ray distribution for each direction. Therefore, the ray tracing is performed only for different cell types. This scheme significantly reduces the computer memory and the computing time in the ray tracing. It must be also noted that with this modified scheme, the rays on reflective or external boundaries can return to the exactly same position. The numerical tests of the acceleration and parallelization methods for several multigroup fuel assembly problems and a whole core problem show that they are effective in terms of the reduction of the number of iterations and the computing time and that the CRX code can be effectively used to accurately solve the large scale heterogeneous transport problems.

II. THEORY AND METHODOLOGY

II.1 The Methodology of the CRX Code

To describe the method of characteristics, the starting equation is the within-group transport equation in discrete ordinates form :

$$\left[\hat{\Omega}_n \cdot \vec{\nabla} + \sigma_g(\vec{r})\right] \psi_g(\vec{r}, \hat{\Omega}_n) = \sum_{g'=1}^{G} \sum_{l=0}^{L} \sum_{m=-l}^{l} Y_{ml}(\hat{\Omega}_n) \sigma_{slgg'}(\vec{r}) \phi_{lg'}^{m}(\vec{r}) + \frac{\chi_g}{k_{eff}} \sum_{g'=1}^{G} (\nu\sigma_f)_{g'} \phi_{g'} = q_{g,n} \tag{1}$$

where w_n is the weight for direction $\hat{\Omega}_n$, L is the order of anisotropy of scattering (L=3 in

the current version of CRX) and the moments ϕ_{lg}^m are given by

$$\phi_{lg}^m(\vec{r}) = \sum_{n=1}^{N} w_n Y_{ml}^*(\hat{\Omega}_n)\psi_g(\vec{r}, \hat{\Omega}_n), \tag{2}$$

where N is the number of directions. Eq.(1) can be rewritten in the following differential form :

$$\sin\theta_n \frac{d\psi_{g,n}}{dp} + \sigma_g \psi_{g,n} = q_{g,n}, \tag{3}$$

where p is the projected coordinate on $x-y$ plane of the coordinate along the neutron trajectory for direction $\hat{\Omega}_n$ and θ_n is the polar angle. The equation for the outgoing flux along a ray in a computational mesh with the flat source approximation is obtained by analytically integrating Eq.(3) :

$$\psi_{g,n,l}^{out} = \psi_{g,n,l}^{in} e^{-\sigma_g L_{n,l}/\sin\theta_n} + \frac{q_{g,n}}{\sigma_g}(1 - e^{-\sigma_g L_{n,l}/\sin\theta_n}), \tag{4}$$

where $L_{n,l}$ is the track length of the l'th ray for direction $\hat{\Omega}_n$ in the mesh. The average flux along the ray included in the mesh for direction $\hat{\Omega}_n$ is obtained by integrating Eq.(3). The equation is given as follows :

$$\bar{\psi}_{g,n,l} = \frac{q_{g,n}}{\sigma_g} + \sin\theta_n \frac{(\psi_{g,n,l}^{in} - \psi_{g,n,l}^{out})}{\sigma_g L_{n,l}}. \tag{5}$$

However, to perform the scattering source iteration, the average angular flux over the computational mesh is required for generation of the source. The equation for the average flux over the computational mesh is obtained by summing the average fluxes (Eq.(5)) over the rays passing through the mesh. The equation is given as follows :

$$\bar{\psi}_{g,n} = \frac{q_{g,n}}{\sigma_g} + \frac{\sin\theta_n}{A\sigma_g} \sum_{l \in \text{mesh}(i,j)} \delta_n \left(\psi_{g,n,l}^{in} - \psi_{g,n,l}^{out}\right), \tag{6}$$

where δ_n represents the spacing between two adjacent rays for direction $\hat{\Omega}_n$, and A is the area of the mesh. In the method of characteristics, Eq.(4) and Eq.(6) with a general tracking module are complete for transport calculation.

II.2 Coarse Mesh/Coarse Group Rebalance Method

The balance equation obtained by integrating Eq.(1) is given by

$$\vec{\nabla} \cdot \vec{J}_g(\vec{r}) + \sigma_{rg}(\vec{r})\phi_g(\vec{r}) = S_g(\vec{r}), \tag{7}$$

where $\sigma_{rg} = \sigma_g - \sigma_{sgg}$, $\vec{J}$ is the current vector and $S_g(\vec{r})$ is the integration of the sum of the scattering source from other energy groups, fission source and anisotropic scattering source. The odd order terms of the anisotropic scattering source in $S_g(\vec{r})$ vanish by integration over all directions but the even order terms remain depending on the chosen angular sets. In the third order anisotropy, the following terms remain :

$$S_{g,anisotropic} = \sum_{g'=1}^{G} \sigma_{s2gg'}(\vec{r}) \sum_{n=1}^{N} w_n \left\{ Y_{02}^e(\hat{\Omega}_n)\phi_{2g'}^0(\vec{r}) + 2Y_{22}^e(\hat{\Omega}_n)\phi_{2g'}^2(\vec{r}) \right\}. \tag{8}$$

Then by integrating this equation over coarse mesh $\tilde{V}_m$ and applying divergence theorem, we can rewrite this equation as follows :

$$\sum_{m'} \int_{\Gamma_{mm'}} d\Gamma \hat{n} \cdot \vec{J}_g + \int_{\tilde{V}_m} dV \sigma_{rg} \phi_g = \int_{\tilde{V}_m} dV S_g, \tag{9}$$

where $\Gamma_{mm'}$ is the surface between $\tilde{V}_m$ and $\tilde{V}_{m'}$,and $\hat{n}$ represents unit normal vector of $\Gamma_{mm'}$. Coarse mesh rebalance method requires that the new iterate $\psi_g^{t+1}(\vec{r}, \hat{\Omega}_n)$ must satisfy this balance equation for each cell, and this is accomplished by multiplying the unaccelerated iterate $\tilde{\psi}_g^t$ by a factor $f_{m,g}$ for each coarse mesh $\tilde{V}_m$:

$$\begin{aligned}
\psi_g^{t+1}(\vec{r}, \hat{\Omega}_n) &= f_{m,g} \tilde{\psi}_g^t(\vec{r}, \hat{\Omega}_n), && \vec{r} \in \tilde{V}_m, \\
\psi_g^{t+1}(\vec{r}, \hat{\Omega}_n) &= f_{m,g} \tilde{\psi}_g^t(\vec{r}, \hat{\Omega}_n), && \vec{r} \in \Gamma_{mm'}, \quad \hat{n} \cdot \hat{\Omega}_n > 0, \\
\psi_g^{t+1}(\vec{r}, \hat{\Omega}_n) &= f_{m',g} \tilde{\psi}_g^t(\vec{r}, \hat{\Omega}_n), && \vec{r} \in \Gamma_{mm'}, \quad \hat{n} \cdot \hat{\Omega}_n < 0.
\end{aligned} \tag{10}$$

We can rewrite Eq.(9) using Eq.(10) as follows :

$$\begin{aligned}
\left[\int_{\tilde{V}_m} dV \sigma_{rg} \tilde{\phi}_g^t + \sum_{m'} \int_{\Gamma_{mm'}} d\Gamma \tilde{J}_{g+}^t - \mathrm{S.A}_g \right] f_{m,g} - \sum_{m'} \int_{\Gamma_{mm'}} d\Gamma \tilde{J}_{g-}^t f_{m',g} \\
= \int_{\tilde{V}_m} dV \left[\frac{\chi_g}{k_{eff}} \mathrm{F.S} + \mathrm{I.S}_g + \mathrm{A.S}_g \right],
\end{aligned} \tag{11}$$

$$\tilde{\phi}_g^t = \sum_n w_n \tilde{\psi}_g^t(\vec{r}, \hat{\Omega}_n), \tag{12}$$

$$\tilde{J}_{g+}^t = \sum_{\hat{\Omega}_n \cdot \hat{n} > 0} w_n \hat{\Omega}_n \cdot \hat{n} \tilde{\psi}_g^t(\vec{r}, \hat{\Omega}_n), \tag{13}$$

$$\tilde{J}_{g-}^t = \sum_{\hat{\Omega}_n \cdot \hat{n} < 0} w_n |\hat{\Omega}_n \cdot \hat{n}| \tilde{\psi}_g^t(\vec{r}, \hat{\Omega}_n), \tag{14}$$

$$\begin{aligned}
\mathrm{F.S} &= \sum_{g'=1}^{G} (\nu \sigma_f)_{g'} \tilde{\phi}_{g'}^t, \\
\mathrm{I.S}_g &= \sum_{g'=1, g' \neq g}^{G} \sigma_{s0gg'} \tilde{\phi}_{g'}^t, \\
\mathrm{S.A}_g &= \sum_{l=2,even}^{L} \sum_{m=-l,even}^{l} \left\{ \sum_{n=1}^{N} w_n Y_{ml}(\hat{\Omega}_n) \right\} \sigma_{slgg} \tilde{\phi}_{lg}^{m,t}, \\
\mathrm{A.S}_g &= \sum_{g'=1, g' \neq g}^{G} \sum_{l=2,even}^{L} \sum_{m=-l,even}^{l} \left\{ \sum_{n=1}^{N} w_n Y_{ml}(\hat{\Omega}_n) \right\} \sigma_{slgg'} \tilde{\phi}_{lg'}^{m,t},
\end{aligned}$$

where F.S represents fission source, $\mathrm{I.S}_g$ represents isotropic scattering source from other energy groups, $\mathrm{S.A}_g$ represents self group anisotropic scattering source and $\mathrm{A.S}_g$ represents anisotropic scattering source from other energy groups.

In the CRX code, the integrals over the top or bottom cell of Eq.(13) is calculated as follows :

$$\int_{\Gamma_{mm'}} d\Gamma \tilde{J}^t_{g+} = \sum_{l\in\Gamma_{mm'}} \sum_{\hat{\Omega}_n\cdot\hat{n}>0} w_n(\sin\theta_n \sin\varphi_n)\tilde{\psi}^t_g(\delta_n/\sin\varphi_n), \tag{15}$$

and over the left or right cell is calculated as follows :

$$\int_{\Gamma_{mm'}} d\Gamma \tilde{J}^t_{g+} = \sum_{l\in\Gamma_{mm'}} \sum_{\hat{\Omega}_n\cdot\hat{n}>0} w_n(\sin\theta_n \cos\varphi_n)\tilde{\psi}^t_g(\delta_n/\cos\varphi_n). \tag{16}$$

To close the rebalance equation (Eq.(11)), the current continuity relations are used to obtain incoming current.

For an eigenvalue problem, Eq.(11) can be expressed as follows :

$$\begin{aligned}\left[\int_{\tilde{V}_m} dV\sigma_{rg}\tilde{\phi}^k_g + \sum_{m'}\int_{\Gamma_{mm'}} d\Gamma \tilde{J}^k_{g+} - \mathrm{S.A}_{\mathrm{o}g}\right] f_{m,g} - \sum_{m'}\int_{\Gamma_{mm'}} d\Gamma \tilde{J}^k_{g-} f_{m',g} \\ = \int_{\tilde{V}_m} dV\left[\frac{\chi_g}{k_{eff}}\mathrm{F.S_o} + \mathrm{I.S}_{\mathrm{o}g} + \mathrm{A.S}_{\mathrm{o}g}\right],\end{aligned} \tag{17}$$

$$\begin{aligned}\mathrm{F.S_o} &= \sum_{g'=1}^{G}(\nu\sigma_f)_{g'}\tilde{\phi}^k_{g'} f_{m,g'},\\ \mathrm{I.S}_{\mathrm{o}g} &= \sum_{g'=1,g'\neq g}^{G}\sigma_{s0gg'}\tilde{\phi}^k_{g'} f_{m,g'},\\ \mathrm{S.A}_{\mathrm{o}g} &= \sum_{l=2,even}^{L}\sum_{m=-l,even}^{l}\left\{\sum_{n=1}^{N} w_n Y_{ml}(\hat{\Omega}_n)\right\}\sigma_{slgg}\tilde{\phi}^{m,k}_{lg},\\ \mathrm{A.S}_{\mathrm{o}g} &= \sum_{g'=1,g'\neq g}^{G}\sum_{l=2,even}^{L}\sum_{m=-l,even}^{l}\left\{\sum_{n=1}^{N} w_n Y_{ml}(\hat{\Omega}_n)\right\}\sigma_{slgg'}\tilde{\phi}^{m,k}_{lg'} f_{m,g'},\end{aligned}$$

where k is the outer iteration index.

Summing Eq.(17) over a coarse energy group (g_c) with the assumption that the rebalance factor is common in the coarse energy group g_c gives the following equation :

$$\begin{aligned}\sum_{g\in g_c}\left[\int_{\tilde{V}_m} dV\left\{\sigma_g\tilde{\phi}^k_g - \sum_{g'\in g_c}\sigma_{s0gg'}\tilde{\phi}^k_{g'}\right\} + \sum_{m'}\int_{\Gamma_{mm'}} d\Gamma\tilde{J}^k_{g+} - \mathrm{S.A}_{\mathrm{c}g}\right] f_{m,g_c} \\ - \sum_{g\in g_c}\sum_{m'}\int_{\Gamma_{mm'}} d\Gamma\tilde{J}^k_{g-} f_{m',g_c} = \sum_{g\in g_c}\left[\frac{\chi_g}{k_{eff}}\int_{\tilde{V}_m} dV(\mathrm{F.S_c}) + \int_{\tilde{V}_m} dV\left(\mathrm{I.S}_{\mathrm{c}g} + \mathrm{A.S}_{\mathrm{c}g}\right)\right],\end{aligned} \tag{18}$$

$$
\begin{aligned}
\mathrm{F.S}_c &= \sum_{g'_c=1}^{G_c} \sum_{g' \in g'_c} (\nu\sigma_f)_{g'} \tilde{\phi}^k_{g'} f_{m,g'_c}, \\
\mathrm{I.S}_{cg} &= \sum_{g'_c=1, g'_c \neq g_c}^{G_c} \sum_{g' \in g'_c} \sigma_{s0gg'} \tilde{\phi}^k_{g'} f_{m,g'_c}, \\
\mathrm{S.A}_{cg} &= \sum_{g' \in g_c} \sum_{l=2,even}^{L} \sum_{m=-l,even}^{l} \left\{ \sum_{n=1}^{N} w_n Y_{ml}(\hat{\Omega}_n) \right\} \sigma_{slgg'} \tilde{\phi}^{m,k}_{lg'}, \\
\mathrm{A.S}_{cg} &= \sum_{g'_c=1, g'_c \neq g_c}^{G_c} \sum_{g' \in g'_c} \sum_{l=2,even}^{L} \sum_{m=-l,even}^{l} \left\{ \sum_{n=1}^{N} w_n Y_{ml}(\hat{\Omega}_n) \right\} \sigma_{slgg'} \tilde{\phi}^{m,k}_{lg'} f_{m,g'_c},
\end{aligned}
$$

where G_c is the number of coarse energy groups. This equation looks like the finite differenced equation of the multigroup diffusion equation involved with the eigenvalue. Therefore, this equation is solved iteratively.

Although this coarse mesh rebalance method is very easy to implement to accelerate various transport calculation methods and the computational cost in solving the rebalance equation is very small, it must be carefully applied to practical problems since it can be unstable or very ineffective in reducing the computing time. A theoretical analysis of the stability was performed for the S_N method by Cefus and Larsen [17] using Fourier analysis through the linearization procedure. The CMR method becomes less efficient or possibly unstable as the scattering ratio increases to unity (the thermal energy groups in water region have the scattering ratio very close to unity). Also, the efficiency of CMR depends strongly on the mesh size and the number of fine meshes in a coarse mesh. As the number of fine meshes in a coarse mesh increases, the stability of CMR increases but its effectiveness decreases.

II.3 Whole-Core Heterogeneous Calculation

In the original ray tracing scheme of the CRX code, the ray tracing is performed over the whole problem and the computed neutron track lengths for all azimuthal directions and for the whole problem are stored for use in the scattering source iteration. Therefore, the scheme can treat any angular quadrature set and any geometrical structure of the problem, although it would require large computer memory and consume long computing time for large scale problems such as the whole-core heterogeneous calculation. Thus, the scheme can be very ineffective for large scale problems that are comprised of lattice cells even with the same geometric dimensions. Therefore, we have modified the scheme to modular ray tracing so that the ray tracing can be performed only for different geometrical cell types and therefore, the computing time and computer memory are reduced significantly in the ray tracing. First, the sizes of the lattice cells are assumed to be the same. In order for all lattice cells to have the same ray distribution, the angular azimuthal quadrature set ([18], [19], see Figure 1) proposed by Filippone *et al* is selected. The azimuthal angles (φ) for first octant are determined by

$$
tan(\varphi_r) = (A/B) \times \frac{r}{(N_\varphi + 1 - r)}, \; r = 1, 2, 3, \cdots, N_\varphi, \tag{19}
$$

where N_φ is the number of azimuthal angles for first octant, A and B are the sizes of the lattice cell for x and y directions, respectively. Then, the number of rays for each direction in a lattice cell is equal to $N_\varphi + 1$. Therefore, if the number of rays for one lattice cell is

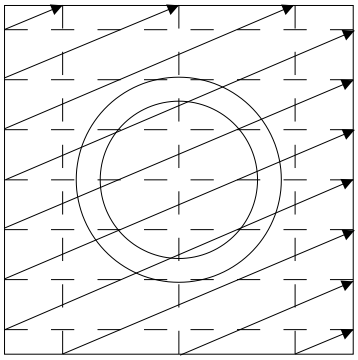

(a) Ray distribution when r=3

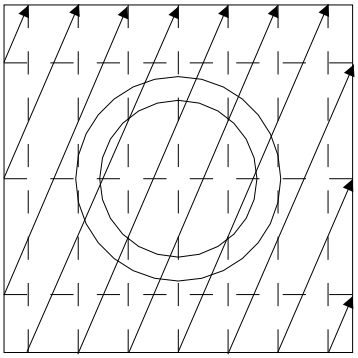

(b) Ray distribution when r=7

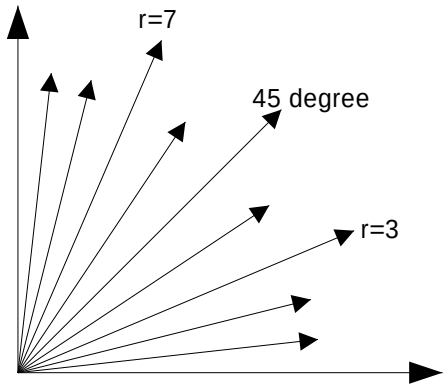

(c) Azimuthal angles (N_φ=9, N'_φ=2)

Figure 1: Ray distributions and azimuthal directions

specified, the number of azimuthal angles for an octant is determined. The number of rays used is typically more than 20. Therefore, the number of azimuthal angles is too large and it may lead to very long computing time. Thus, we use only a subset (N'_φ) of these angles selected by considering the symmetry about the 45 degree line (see Figure 1). With this scheme, the ray distributions for all lattice cells become the same. Another merit of this angular quadrature set is the improvement of the accuracy due to the return of the rays to the exactly same position on the reflective or external boundaries.

Furthermore, the rays are swept through the whole problem domain, e.g., starting from an external boundary, reflecting at a reflective boundary (if any), and then ending at an external boundary.

II.4 Parallel Computation

Parallel computation of the CRX code was performed with MPI (Message Passing Interface). The message passing model posits a set of processors that have only local memory but

are able to communicate with other processors by sending and receiving messages. The sum of angular fluxes, rebalance factors, and flux moments are transferred. Each processor calculates for $N_{angle}/N_{processor}$ directions. So each computer has the following calculated results :

$$\phi_{lg}^{m,P}(\vec{r}) = \sum_{n=1}^{n\in n_P} w_n Y_{ml}^*(\hat{\Omega}_n)\psi_g(\vec{r},\hat{\Omega}_n), \tag{20}$$

where P represents the processor number, and n_P represents the angle set which is calculated in processor P. After this procedure, the above data are collected and summed as follows :

$$\phi_{lg}^{m}(\vec{r}) = \sum_{P} \phi_{lg}^{m,P}(\vec{r}). \tag{21}$$

Then these results are distributed to each processor for next iteration. Then leakage terms are collected to calculate rebalance factors in master processor (one of the processors). These rebalanced factors are then distributed to each processor and multiplied to all of the flux moments in each processor.

The ray sweeping strategy in Section II.3 with the angularly decomposed parallel computation does not require iteration on the assumed interface angular fluxes, in contrast to the domain decomposition parallel scheme in Ref. [13].

The efficiency of this parallel computation depends on the number of computational meshes since the communication time increases as the number of meshes increases (in our scheme, the amount of communication is proportional to the number of meshes). This method is effective in problems in which the communication time is a small portion of the total time (i.e., communication time plus computing time). The Calculational procedures of the CMR/CGR acceleration and parallelization are shown in Figure 2.

III. NUMERICAL RESULTS

We solved several problems to test the CMR/CGR acceleration efficiency. In the following tables, the notation CRX(a, b, c) represents that the test was performed under a angular divisions in azimuthal direction, b angular divisions in polar direction and c rays in each direction over the problem domain.

To show the effectiveness of CMR for isotropic scattering, we chose BWR 4x4 (Figure 3) and BWR 7x7 assembly problems. We accelerated the outer iteration of these problems by applying CMR/CGR (all-group-collapsed, coarse group, and group-wise rebalance) methods. In coarse group rebalance method, we grouped multigroups into two coarse groups. The notation CGR$[1, g]$ in Table 1 represents that the groups from group 1 to group $g-1$ were grouped into the first coarse group and the groups from group g to group G were grouped into the second coarse energy group.

For these problems, the convergence criterion of 10^{-6} for eigenvalue and fission source was used. Reflective boundary conditions were applied to all boundaries in these problems. The 4x4 BWR problem consists of 16 fuel pins (14 identical UO_2 fuel cells and 2 gadolinium poisoned ones). It is a seven-group eigenvalue problem and has upscattering in group 5, 6, and 7.

In Table 1, speedup-P represents the ratio of the computing time without parallel computation to the computing time with parallel computation, and speedup-T represents the total

Table 1: Results of BWR 4x4 (7 Groups), CRX(8,3,600)

	Computing time[a] (sec)	Speedup-P	Speedup-T
No acceleration	2897.36	-	1.0
CMR/CGR-A	734.26	-	3.95
CMR/CGR[1,3]	501.40	-	5.78
CMR/CGR-G(1[b])	460.83	1.0	6.29
CMR/CGR-G(2)	231.41	1.99	12.52
CMR/CGR-G(3)	155.64	2.96	18.62
CMR/CGR-G(4)	118.31	3.90	24.53
CMR/CGR-G(6)	80.08	5.75	36.15
CMR/CGR-G(8)	61.95	7.43	46.73
CMR/CGR-G(12)	42.82	10.76	67.68

[a] on KAIST*GALAXY cluster
(16 Pentium II 300MHz computers, 100Mbps bandwidth, 100 μsec latency)
[b] number of CPUs
k_{eff}=1.01060

speedup with acceleration and parallel computing, (i.e., speedup-A $\times$ speedup-P). CGR-A represents all-group-collapsed CMR and CGR-G represents group-wise CMR.

The results for the BWR 4x4 problem are given in Table 1. The coarse mesh group-wise rebalance method also shows the best results in this test problem. The results show that the number of iterations and the computing time are reduced as the number of coarse energy groups (i.e., g_c) increases. Therefore , the group-wise rebalance method is best in comparison with others. This reason is due to the fact that for problems with significant upscattering the group-wise rebalance method gives the most detail description of the energy dependence of the rebalance factor and the computing time for solving the rebalance equation is relatively short compared to the total computing time. Parallel computation also seems very effective in this problem. In the results, the efficiency of parallel computation, (i.e., speedup-P/(# of CPUs)), is reduced gradually when the number of CPUs is increased. This is because there exists communication time. The communication time does not change as the number of CPUs changes, but computing time in each computer changes. So the ratio with computing time and communication is reduced when the number of CPUs is increased.

Table 2: Results of BWR 7x7 (2 Groups) Without Upscattering, CRX(4,4,400)

Order of anisotropy		Computing time (s)	Speedup-A	k_{eff}
0	No acceleration	468.57	1.00	1.02863
	CMR/CGR-A	67.95	6.90	
	CMR/CGR-G	70.48	6.65	
1	No acceleration	489.23	1.00	1.02797
	CMR/CGR-A	66.57	7.35	
	CMR/CGR-G	67.88	7.21	
3	No acceleration	598.42	1.00	1.02842
	CMR/CGR-A	81.47	7.35	
	CMR/CGR-G	81.56	7.34	

To test efficiency of acceleration in problems with highly anisotropic scattering, the 7x7 BWR fuel assembly problem in Ref. [20] (Figure 4) was selected and modified. The isotropic components of the cross section data are described in Ref. [20]. Water gaps and assembly walls in the original problem were removed and anisotropic scattering cross sections whose values are a tenth of the isotropic scattering cross sections were added. This problem is a two-group eigenvalue problem and consists of 7x7 homogenized fuel cells. Reflective boundary conditions were used on all boundaries. The results are shown in Table 2. This problem does not have upscattering. Thus the significant difference between the efficiency of acceleration of all-group-collapsed CGR and of group-wise CGR does not appear. The speedup is about $6 \sim 7$.

To test whole-core heterogeneous calculation, we made a 4x4 small 1/4 core problem (Figure 6). Each assembly of this problem consists of 17x17 lattices (Figure 5). The problem is a 7 group isotropic scattering problem but with no upscattering. 3x3 coarse meshes per assembly were used to apply CMR acceleration. The convergence criteria of 10^{-6} for eigenvalue and 10^{-5} for fission source were used.

Table 3: Results of the 1/4 Core Problem (7 Groups), CRX(4,2,1632)

	Computing time (sec)	Speedup-P	Speedup-T
No acceleration	212662.8	-	1.0
CMR/CGR-G(1^a)	31311.15	1.0	6.79
CMR/CGR-A(1)	22100.3	1.0	9.62
CMR/CGR-G(4)	8529.7	3.67	24.93
CMR/CGR-A(4)	5938.8	3.72	35.81
CMR/CGR-G(8)	4658.2	6.72	45.65
CMR/CGR-A(8)	3210.3	6.88	66.24

[a] number of CPUs
k_{eff}=1.03027

Table 4: Normalized Assembly Power Distribution

1.761	0.478	
0.796	0.817	0.478
1.113	0.796	1.761

The results are shown in Table 3. In this problem, all-group-collapsed CMR was very effective compared with the previous problems and was even more effective than the groupwise CMR. This problem exhibits very slow convergence in thermal groups and takes too much time without acceleration and parallelization. Therefore, the acceleration and parallel computing

have significant importance. For this problem, total speedup using the all-group-collapsed CMR and using 8 processors is 66.24 and the computing time is 3210 sec.

Table 4 and Figure 7 show normalized assembly power distribution and cell averaged flux, respectively.

IV. CONCLUSIONS

The method of characteristics in the CRX code extended to anisotropic scattering was accelerated with the coarse mesh rebalance (CMR) method for inner iteration and the coarse mesh/coarse group rebalance method for outer iteration. Parallel computation with an angular decomposition was also implemented to further reduce the computing time and computer memory. The results show that the group-wise coarse mesh rebalance method is the most effective in tested problems having upscattering, while the all-group-collapsed CMR appears to be effective for problems having downscattering only. The speedup achieved by the acceleration is typically $3 \sim 10$, and by the parallel computation about $6 \sim 7$ with 8 CPUs. By applying both acceleration and parallel computation, the computing time of the method of characteristics is significantly reduced, with speedup on the order of $20 \sim 60$.

To effectively handle heterogeneous large scale problems, including the multi-assembly problems and the whole core problems, the original ray tracing scheme was modified so that all lattice cells have the same ray distributions for each direction. With this modular ray tracing scheme, the ray tracing is performed only for geometrically different cell types and therefore, the computer memory and computing time in ray tracing are significantly reduced. Further, this scheme improves the accuracy by the rays returning to the the exactly same position on the reflective or external boundaries. Since the rays are swept through the whole problem domain, the parallel computation based on angular decomposition does not require iteration on the interface angular fluxes, thus also leading to the reduction of computing time.

References

[1] N. Z. Cho and S. G. Hong, "CRX : A Transport Theory Code for Cell and Assembly Calculations Based on Characteristic Method," *Proc. International Conf. on the Physics of Reactors*, September 16-20, Mito, Japan, Vol. 1A, p.250, 1996.

[2] S. G. Hong and N. Z. Cho, "CRX : A Code for Rectangular and Hexagonal Lattices Based on the Method of Characteristics," *Annals of Nuclear Energy*, **25**, 547, 1998.

[3] M. J. Halsall, "CACTUS, A Characteristics Solutions to the Neutron Transport Equations in Complicated Geometries," AEEW-R-1291, U.K. Atomic Energy Authority, 1980.

[4] M. D. Brough and C. T. Chudley, "Characteristic Ray Solutions of the Transport Equation," *Advances in Nuclear Science an Technology*, Vol. 12, Plenum Press, New York,1980.

[5] L. Goldberg, J. Vujic, A. Leonard, and R. Stachowski, "The Characteristics Method in General Geometry," *Trans. Am. Nucl. Soc.*, **112**, 16, 1992.

[6] R. Roy, "The Cyclic Characteristics Method with Anisotropic Scattering," *Proc. Int. Conf. Mathematics and Computation, Reactor Physics and Environmental Analysis in Nuclear Applications*, p.1225, Madrid, Spain, September 27-30, 1999.

[7] R. E. Alcouffe and E. W. Larsen, "A Review of Characteristic Methods Used to Solve the Linear Transport Equations," *Proc. Int. Topl. Advances in Mathematical Methods for the*

Solution of Nuclear Engineering Problems, Munich, FRG, April 27-29, 1981, American Nuclear Society, 1981.

[8] S. G. Hong and N. Z. Cho, "Method of Characteristic Direction Probabilities for Heterogeneous Lattice Calculation," *Nuclear Science and Engineering*, **132**, 65-77, 1999.

[9] R. E. Alcouffe, "Diffusion Synthetic Acceleration Methods for the Diamond Differenced Discrete Ordinates Equations," *Nuclear Science and Engineering*, **64**, 344, 1977.

[10] M. L. Adams and W. R. Martin, "Boundary Projection Acceleration : A New Approach to Synthetic Acceleration of Transport Calculation," *Nuclear Science and Engineering*, **100**, 177, 1988.

[11] S. G. Hong and N. Z. Cho, "A Rebalance Approach to Nonlinear Iteration for Solving the Neutron Transport Equations," *Annals of Nuclear Energy*, **24**, 147, 1997.

[12] E. W. Larsen, "Unconditionally Stable Diffusion Synthetic Acceleration Methods for the Slab Geometry Discrete Ordinates Equations. Part I : Theory," *Nuclear Science and Engineering*, **82**, 47, 1982.

[13] S. Kosaka and E. Saji, "The Characteristics Transport Calculation for a Multi-Assembly System Using Neutron Path Linking Technique," *Proc. Int. Conf. Mathematics and Computation, Reactor Physics and Environmental Analysis in Nuclear Applications*, p.1890, Madrid, Spain, September 27-30, 1999.

[14] E. E. Lewis and W. F. Miller, Jr., "Computational Methods of Neutron Transport," John Wiley & Sons, 1984.

[15] R. E. Alcouffe and R. D. O'Dell, "Tranport Calculations for Nuclear Reactors," CRC Handbook of Nuclear Reactor Calculation, Edited by Y. Ronen, CRC Press, 1986.

[16] G. S. Lee, "Parallelization and Coarse Mesh Rebalance Acceleration of the Method of Characteristics in Neutron Transport Theory," M.S. Thesis, KAIST, 2000.

[17] G. R. Cefus and E. W. Larsen, "Stability Analysis of Coarse-Mesh Rebalance," *Nuclear Science and Engineering*, **105**, 31, 1990.

[18] W. L. Filippone, S. Woolf, and R. J. Lavigne, "Particle Transport Calculations with the Method of Streaming Rays," *Nuclear Science and Engineering*, **77**, 119, 1981.

[19] S. G. Hong and N. Z. Cho, "Extension of Streaming Rays Method for Streaming Dominant Neutron Transport Problems," *Journal of Korean Nuclear Society*, **28**, 320, 1996.

[20] G. Ball and Z. Weiss, *Annals of Nuclear Energy*, **20**, 59-70, 1993

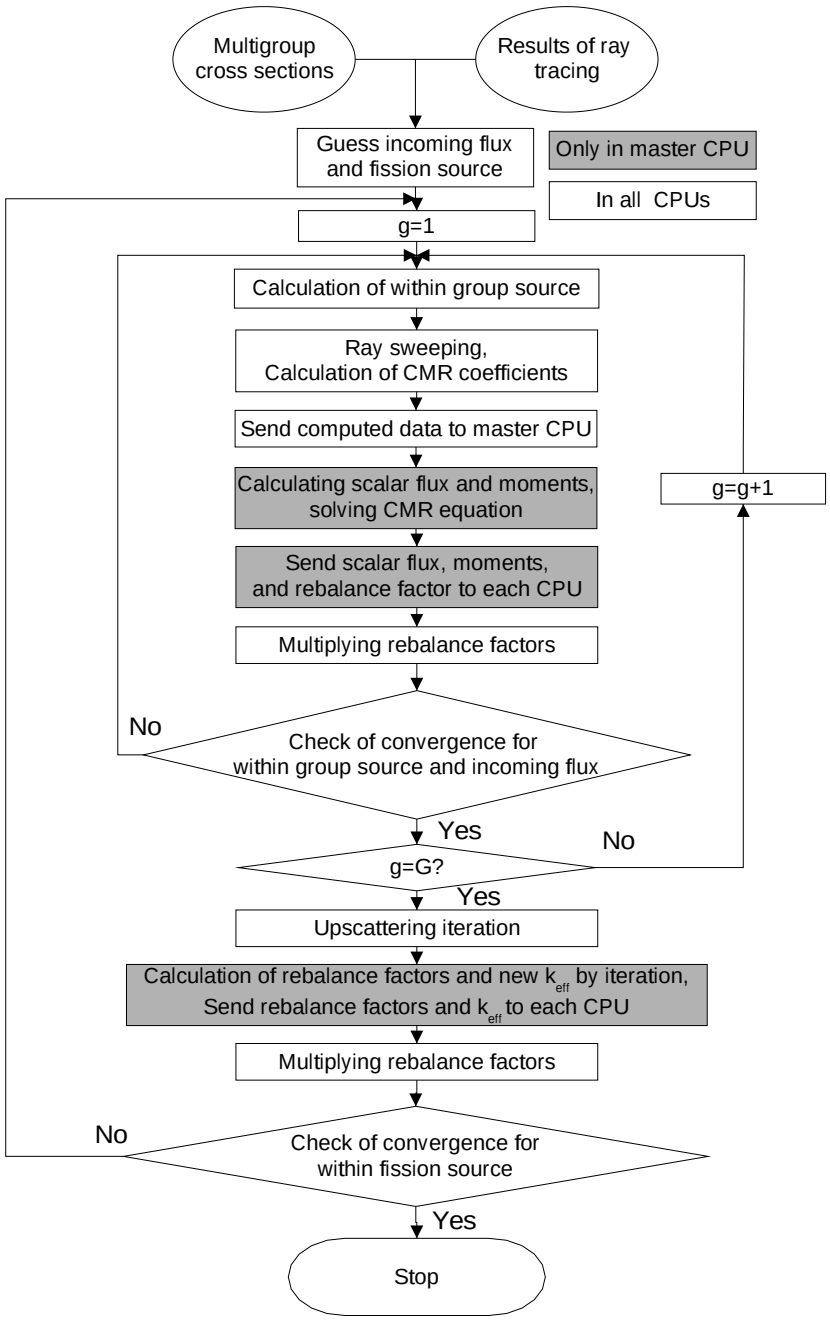

Figure 2: Flow Chart of the CMR/CGR-Accelerated and Parallelized CRX Algorithm

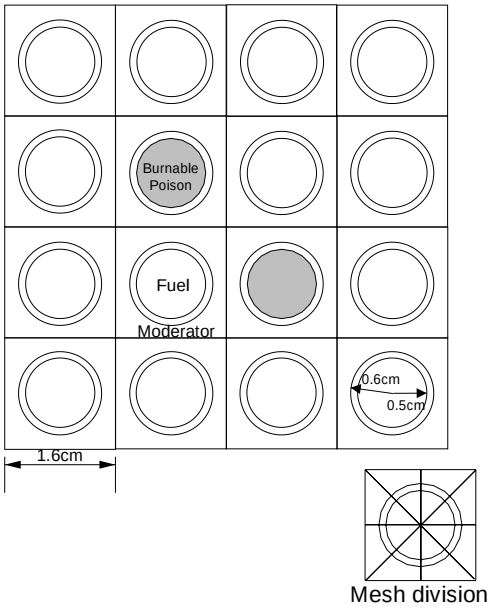

Figure 3: Configuration of 4x4 BWR

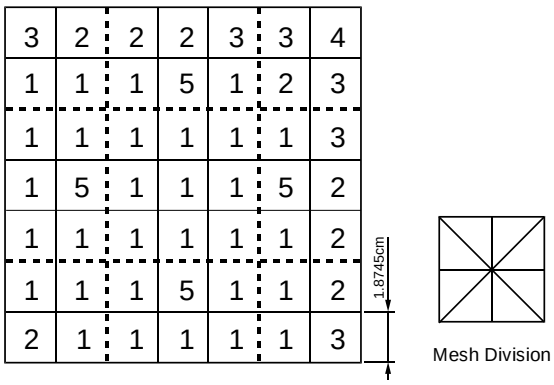

Figure 4: Configuration of 7x7 BWR Fuel Assembly

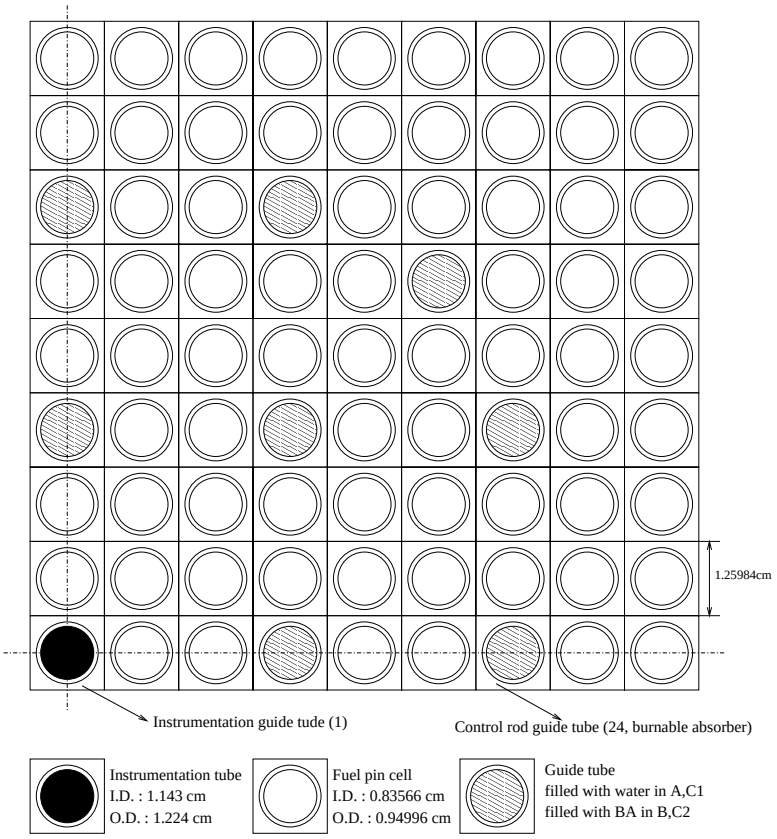

Figure 5: Configuration of 1/4 Fuel Assembly for the 1/4 Core Problem

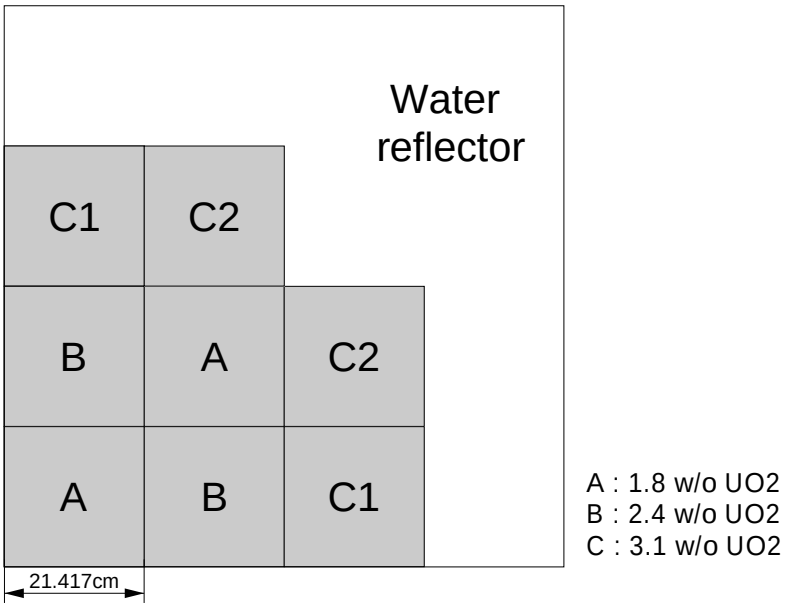

Figure 6: Configuration of the 1/4 Core Problem

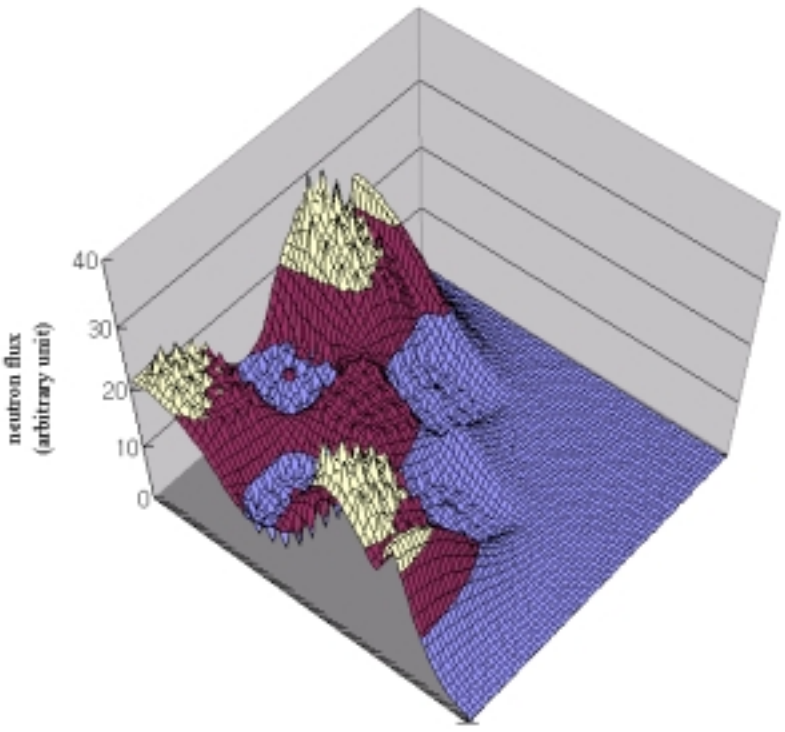

Figure 7: Cell Averaged Neutron Flux Distribution for Group 7